Numerical and Experimental Study of a Concentrated Indentation Force on Polymer Matrix Composites

V.Antonucci*[1,2], M.Esposito[1], R.Marzella[2], and M.Giordano[1,2]
[1]Institute for Composite and Biomedical Materials, CNR,
[2]Imast - Technological District on Polymeric and Composite Engineering Structures
*P.le Enrico Fermi,1 80055 Portici – Italy, vinanton@unina.it

Abstract: A quasi static indentation test on a laminate composite has been investigated numerically and experimentally. In particular, the test has been implemented by Comsol Multiphysics and optimizing the FE element and mesh. In addition, the numerical strain results have been validated by the comparison with the respective experimental deformation data that have been obtained by fiber Bragg grating sensors preliminary embedded within the composite laminate.

Keywords: polymer composite, damage resistance, Fiber Bragg sensors.

1. Introduction

Polymer based composite materials have significant interest and find several engineering applications in many industrial sectors, such as automotive, aeronautic, civil, naval. The optimal design of composite structures requires the use of numerical tools able to perform accurate stress analysis and predict the mechanical behaviour under specified load conditions. Therefore, laminated composite plates and shell elements are available in most of commercial finite-element codes in order to simulate the composite nature.

However, the proper modelling of laminated composites is a not trivial task and can be considered as an open research problem due to the complex and anisotropic behaviour of composites. In order to assess the validity of FE models, it should be useful the measurement of interlaminar deformations during a specified mechanical test.

In this study, the mechanical behaviour of a composite plate under the action of a concentrated indentation force has been investigated both numerically and experimentally.

In particular, the mechanical test described in the ASTM D6264 standard “Standard Test Method for Measuring Damage Resistance of Fiber-Reinforced Polymer-Matrix Composite to Concentrated Quasi-Static Indentation Force” has been implemented.

The analyzed test consists of slowly (1 mm/min) applying an indentation force by pressing a displacement-controlled hemispherical indenter into the face of the specimen (figure 1). The indenter has a smooth hemispherical tip with a diameter of 12.7mm, while the fixture consists of a single plate with a 127.0 mm diameter opening. The specimen is 152 mm square and about 3 mm thick. It is placed directly on the flat rigid support that is mounted in the lower head of the testing machine.

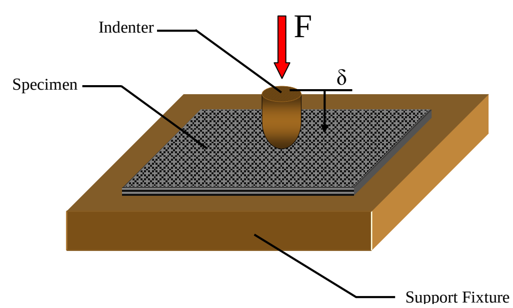

Figure 1. Schematic of the indentation test.

The numerical simulations have been performed by Comsol Multiphysic and modelling the composite laminate as composed of different layers with orthotropic properties. The numerical deformations evaluated in specific positions of the FE model have been compared with experimental deformation data that have been measured by embedded fiber optic Bragg sensors within the composite.

2. FE Model

The FE simulations have been performed by considering a laminate of 6 plies (90°-90°-0°-0°-90°-90°). The global model consists of three domains: composite panel, indenter and plate (see figure 2).

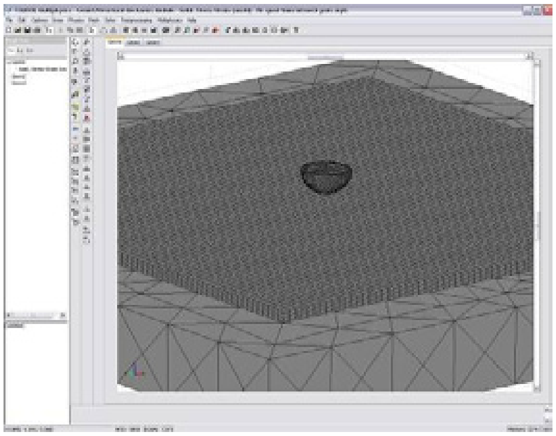

Figure 2. FE mesh

A quadrangular mesh (see figure 2) with an edge of 2 mm and solid element have been adopted. Both the entire whole and ¼ structure have been modelled. In addition, for the entire structure the influence of Not geometrical linearity (NLG) has been investigated.
The lamina properties have been defined by using two reference systems: one for the even layers and one for the odd layers. The independent values of lamina properties have been assigned respect with these reference systems. In particular, the values of the lamina properties have been measured experimentally by proper characterization tests on composites produced with a commercial polyester resin and an unidirectional glass fiber reinforcement and having a fiber volume fraction around 49%. The tests have been performed according with the ASTM standards (D3039 and D3518) in order to evaluate the 0° and 90° elastic moduli, the shear modulus and the Poisson coefficients ν_{12} e ν_{21}.
Table 1 reports the mechanical properties obtained by the experimental characterization.

Mechanical property	**Value**
Elastic modulus E_1	37.09 (GPa)
Elastic modulus E_2	7.35 (GPa)
Poisson coefficient ν_{12}	0.185
Poisson coefficient ν_{21}	0.034
Shear modulus G_{12}	3.14 (GPa)
Tensile strength	660.29(MPa)
Tensile strength	73.19(MPa)
Maximum Shear Stress	44.07(MPa)

Table 1. Experimental lamina mechanical properties.

These results agree with the values obtainable by micromechanics formula for composite materials.
The mesh of the composite laminate has been divided in nine zones in order to increase the element number in the central area where there is the contact with the indenter. The contact has been considered by defining the master and slave surfaces in order to ensure the non penetrability along the contact areas.

3. Numerical results

The numerical results have been compared in terms of the vertices rise and the interlaminar deformation at the points where the Fiber Bragg sensors have been located. In particular, the deformations have been evaluated along the fiber direction between the first and second ply and between the fifth and sixth ply at the center of the laminate quarter (see figure 3).

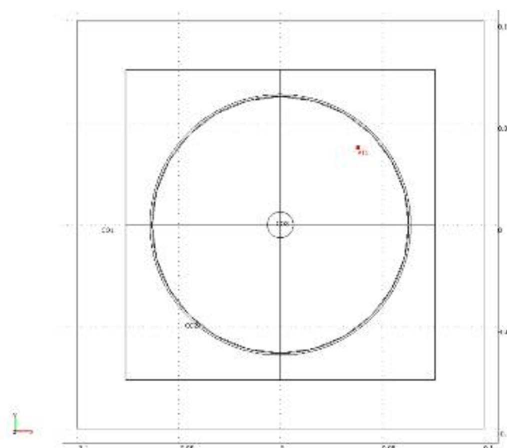

Figure 3. Red point where the deformation are evaluated.

Struct.	N.L.G.	Vertex displacement mm	Deformation ($*10^{-6}$)	
			1°/2°	5°/6°
Entire	Off	1.532	506	- 510
	On	1.476	428	- 525
1/4	Off	1.532	569	- 573
	On	n.d.	n.d.	n.d.

Table 2 . Simulation results

The results shown in table 2 evidence that, when the N.L.G. option is activated, the vertex rise is lower and there is non symmetry for the deformations. In fact the tensile deformations are lower than the compression. For completeness figures 4 and 5 show the deformation map along the fiber direction between the 1° and 2° ply, and between the 5° and 6° ply respectively.

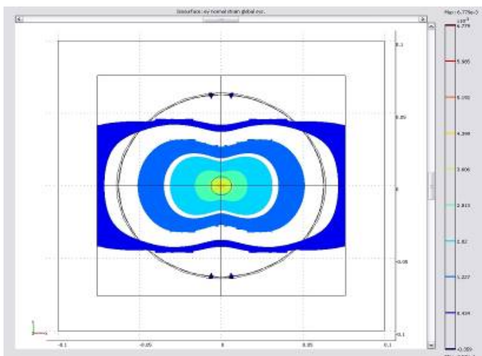

Figure 4. Deformation along the fiber direction between the1° and 2° layers (entire structure)

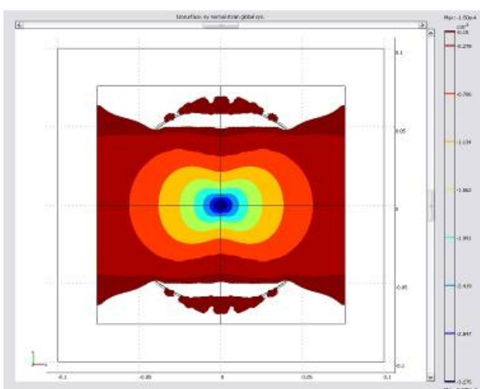

Figure 5. Deformation along the fiber direction between the 5° and 6° layers (entire structure)

4. Experimental

Two composite panels (152*152 mm) of 6 plies (90°-90°-0°-0°-90°-90°) have been produced with the vacuum infusion process. This technology is a low cost process for the manufacturing of continuous fiber reinforced composite materials. It consists of fiber reinforcement impregnation by a thermoset liquid resin that wets the fibers by vacuum application. After the complete impregnation the the composite consolidation occurs by the resin curing reaction.

During the reinforcement lay-up two fiber Bragg gratings sensors (FBG) have been embedded trough the reinforcement between the first and the second ply (denoted with "C" locations) and the five and six ply (denoted with "T" locations). In particular, in the first panel the sensors were located in the positions C1 (33 mm, 40 mm)) and T1 (29 mm, 41 mm, while in the second one in the positions C2 (28 mm, 32 mm) and T2 (33 mm, 28 mm) taking as coordinate reference (0,0) the centre of the laminate. The FBG sensors are tiny sensing elements (few hundreds of μm in diameter) that can be embedded in the body of the product, under examination, without having almost any effect on the stress/strain field transfer between the reinforcement and the polymeric matrix Another great merit of this technique is the capability of being used as an on-line and in-field monitoring method. The main principle on which these sensors operate is very simple, as they act like selective mirrors that reflect a single wavelength, of the light passing in the optic fiber. In fact the Bragg operation relies on grating capability to reflect very narrow-band optical signal at a resonance wavelength λ_B given by:

$$\lambda_B = 2n\Lambda \tag{1}$$

where n is the refractive index of the core, and Λ is the grating pitch. It is well understood that any effect able to modify physical or geometric properties of the grating will lead to a shift in the Bragg resonance wavelength.

The sensor signal has been detected by the MicronOptics sm25 system, having 4 optical channels (80 nm), a resolution of 1 pm, an accuracy of 2 pm, a scan rate of 1 Hz. This instrument is connected to a PC with Labview interface (see figure 6).

The indentation tests have been performed by using the Instron machine 8008 with a loading cell of 100KN. Figure 7 shows a picture of the experimental apparatus and the composite panel, while figure 8 the vertex elevation during the test can be observed.

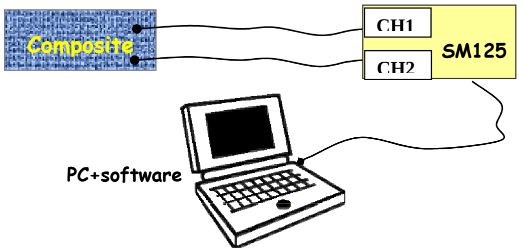

Figure 6. FBG interrogation system set-up

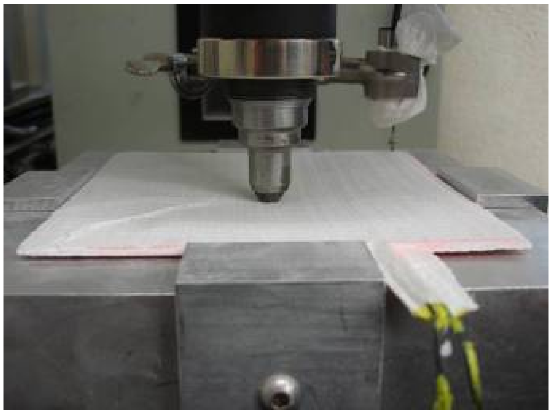

Figure 7. Picture of the experimental apparatus

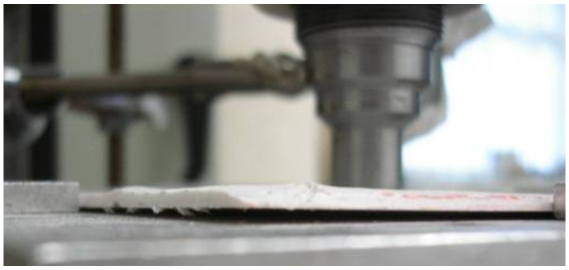

Figure 8. Vertex rise.

Figure 9 reports the measurement of the FBG sensors and the indenter displacement during the indentation test for the first panel. In particular, the FBG measurements are in terms of wavelength. The shift of the wavelength is related to the variations of the deformations.
As expected, the FBG between 1-2 plies (Bragg1-green colour) show compression strain and the FBG between 5-6 plies (Bragg 2- red colour) tensile strain. Similar behaviour has been observed for the second panel.

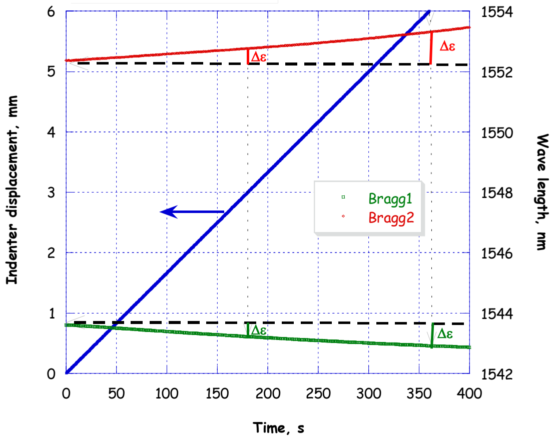

Figure 9. FBG measurement.

5. Experimental-model comparison

The FBG deformation measurements for a displacement of the indenter of 3 mm have been compared with the numerical ones.
Table 3 reports the comparison for both composite panels. The deformation values measured for the composite "2" are than those for the first panel, due to the location of the FBG sensor more close to the indenter area.
The results indicate similar magnitude order for the experimental and numerical data, especially for the first panel. In particular for the first panel the differences are around 20%.

Composite/ position	**Experimental με**	**Numerical με**
1/ply 1-2	396	475
2/ply 1-2	1190	855
1/ply 5-6	-381	-464
2/ply 5-6	-1080	-847

Table 3. Comparison between numerical and experimental deformations.

These differences can be attributed to manufacturing issues, such as the not correct orientation of the composite layers and the FBG position within the reinforcement.

6. References

1. J. Simo and A. Laursen, An augmented Lagrangian treatment of contact problems involving friction, *Computers and Structures* **42**, 97–116 (1992).
2. Standard ASTM D6264